SLOPED ROLLING-TYPE ISOLATION DEVICES FOR SEISMIC PROTECTION OF EQUIPMENT AND FACILITIES

S.J WANG[1*†], J.S. HWANG[2], K.C. CHANG[3], C.Y SHIAU[1] and W.C LIN[1]

[1] *Division of Structural Control, National Center for Research on Earthquake Engineering, Taiwan*

[2] *Department of Construction Engineering, National Taiwan University of Science and Technology, Taiwan*

[3] *Department of Civil Engineering, National Taiwan University, Taiwan*

ABSTRACT

The rolling motion of mutually orthogonal rollers respectively sandwiched between two opposite bearing plates in which one or both are V-shaped sloping surfaces makes the sloped rolling-type isolation device have an excellent in-plane seismic isolation performance. In this study, first, the dynamic behavior of the isolation device with multi-roller and built-in damping mechanisms is discussed. Based on the theoretical derivation results, a simplified mathematical hysteretic model is proposed to characterize the twin-flag hysteresis behavior of the isolation devices with and without built-in damping mechanisms. Secondly, seismic simulation tests on the isolation devices with different design parameters and an isolated raised floor system were conducted. Not only the efficiency of the bearings in protecting objects but also the validation of the derived theory in predicting the seismic responses of the bearings is experimentally demonstrated.

Keywords: Seismic isolation, Sloped multi-roller isolation device, Equipment, Twin-flag hysteresis behavior, Shake table test.

1. INTRODUCTION

The performance-based design for building structures has attracted immense attention in earthquake engineering communities. It is especially emphasized that the seismic performance of buildings depends on not only the seismic-resistant capability of structural components but also the functionality of nonstructural contents. With most structural elements remaining intact during or after earthquakes, the desired performance of buildings may not be achieved if the housed equipment or facilities are malfunction, shutdown or even damaged (Hwang et al. 2004). The past lessons have caused awareness of enhancing seismic performance for the critical equipment and facilities in the relevant industries and organizations. The implementation of seismic isolation devices to equipment or facilities may be one of the most practical and effective strategies (ISO-Base; CRS) to mitigate the seismic risk. An often seen case is to incorporate seismic isolation

* Corresponding author: Email: sjwang@ncree.narl.org.tw

† Presenter: Email: sjwang@ncree.narl.org.tw

bearings into a raised floor system (Lambrou 1994). Several studies were conducted to develop a robust isolation bearing (Ismail 2009; Lee et al. 2010) to improve uplift and insufficient damping issues for traditional sliding-based and rolling-based bearings. Many recent studies also disclosed that for a better displacement control of passive isolation bearings, active or semi-active control devices were suggested to be incorporated into the isolation system [Lu and Lin 2008].

2. ROLLING-TYPE ISOLATION BEARINGS

The base isolation strategy using free-rolling rods on flat bearing plates for seismic protection of building structures was first theoretically and experimentally studied by Lin (Lin and Hone 1993). Accordingly, several more sophisticated rolling-based isolation devices that have both restoring and self-centering capabilities due to gravity were developed (Jangid and Londhe 1998; Kasalanati et al. 1997). Recently, a new rolling-type isolation device employing rolling motion of one cylindrical roller between two bearing plates with a constant sloping surface (i.e. the sloped rolling-type isolation device) was theoretically and experimentally investigated by Tsai (Tsai et al. 2007) and Lee (Lee et al. 2010) for seismic protection of bridge structures. A refined sloped rolling-type isolation device with multi-roller and built-in damping mechanisms (i.e. the sloped multi-roller isolation device (Wang et al. 2012)), as shown in the schematic drawing of Figure 1, is focused in this study. The isolation device is composed of three bearing plates (denoted as upper, intermediate and lower bearing plates hereafter) and two pairs of mutually orthogonal cylindrical rollers. Both surfaces of the intermediate bearing plate are dual V-shaped sloping, while the upper and lower bearing plates can have dual V-shaped sloping or flat surfaces in contact with the rollers. The rolling mechanisms of two pairs of mutually orthogonal rollers provide the in-plane seismic isolation function. The multi-roller mechanism can make synchronous movement for the rollers in each principle horizontal direction. The adjustable linear spring modules embedded in the side plates can generate required normal forces to supply additional sliding friction forces between the side plates and bearing plates. To prevent undesired instant pounding when the roller passes through the sharp angle of the V-shaped surface, an arc with a fixed curvature radius is provided at the intersection of the two inclines of the V-shaped surface of the bearing plate.

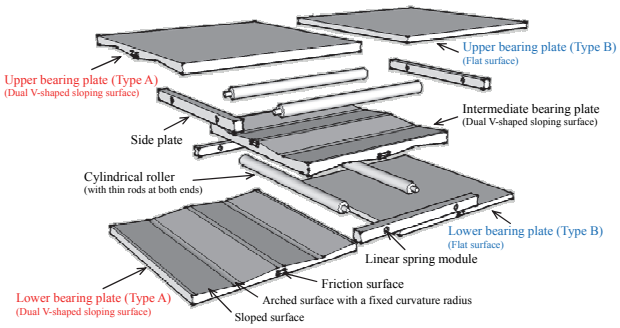

Figure 1: Schematic view of sloped multi-roller isolation devices.

The advantages of the sloped multi-roller isolation device are summarized as follows: (1) the isolation device can offer maximum horizontal decoupling between the protected object and input

excitations since it does not have a fixed vibration natural period; (2) the maximum horizontal acceleration response remains essentially constant regardless of the excitation intensity; (3) the horizontal acceleration transmitted to the protected object can be significantly reduced, since the rolling friction and the restoring force due to gravity of the isolation device are very limited; (4) the isolation device has an efficient inherent gravity-based self-centering capability after excitations; (5) the multi-roller mechanism can effectively prevent sliding motions between rollers and bearing plates, and prevent the isolation device from undesired overturning motions as well; and (6) the built-in damping capability can facilitate the isolation device to suppress excessive displacement responses during excitations, and to stop rolling motion after excitations.

3. MECHANICAL FEATURES AND DYNAMIC BEHAVIOR

3.1. Equations of motion

The following different design features are discussed: (1) rollers move between two V-shaped sloping surfaces, denoted as Type A isolation device hereafter; (2) rollers move between a V-shaped sloping surface and a flat surface, denoted as Type B isolation device hereafter; (3) energy dissipation is only contributed by limited rolling friction; and (4) in addition to rolling friction, the built-in sliding friction damping mechanism is engaged in energy absorption. The equations of motion were derived by Wang (Wang et al. 2012). For Type A isolation device, when the roller is moving within the fixed curvature range, the equation of motion is given by

$$M\ddot{x}_1 + \frac{1}{2R}M(g+\ddot{z}_g)\mathrm{sgn}(x_1)x_1 + (\mu_r N + F_D)\mathrm{sgn}(\dot{x}_1) = -M\ddot{x}_g \tag{1}$$

When the roller is moving apart from the fixed curvature range, it is written as

$$M\ddot{x}_1 + \frac{1}{2}M(g+\ddot{z}_g)\sin 2\theta\,\mathrm{sgn}(x_1) + (\mu_r N + F_D)\cos\theta\,\mathrm{sgn}(\dot{x}_1) = -M\ddot{x}_g \tag{2}$$

For Type B isolation device, when the roller is moving within the fixed curvature range, the equation of motion is given by

$$M\ddot{x}_1 + \frac{1}{4R}M(g+\ddot{z}_g)\mathrm{sgn}(x_1)x_1 + (\mu_r N + F_D)\mathrm{sgn}(\dot{x}_1) = -M\ddot{x}_g \tag{3}$$

When the roller is moving apart from the fixed curvature range, it is written as

$$M\ddot{x}_1 - \frac{1}{2}M(g+\ddot{z}_g)\sin\theta\,\mathrm{sgn}(x_1) + (\mu_r N + F_D)\mathrm{sgn}(\dot{x}_1) = -M\ddot{x}_g \tag{4}$$

where $\ddot{x}_g$ and $\ddot{z}_g$ are respectively the horizontal and vertical acceleration excitations; x_1, $\dot{x}_1$ and

where $\ddot{x}_1$ are the horizontal relative displacement, velocity and acceleration responses of the protected object, respectively; g is the acceleration of gravity; M is the total seismic reactive mass

of the protected object together with the device components; μ_r is the ratio of the rolling resistant coefficient (δ) to the roller radius (r); N is the normal force acting between the bearing plate and roller, which can be approximated by Mg; F_D is the sliding friction force acting parallel to the slope of the bearing plate; R is the curvature radius in the range between two inclines of the V-shaped surface of the bearing plate; and θ is the sloping angle of the V-shaped surface of the bearing plate. More discussions regarding the discrepancy of transmitted acceleration responses between Type A and Type B isolation devices are presented in the follows:

(1) For both isolation devices, when the roller moves apart from the fixed curvature range together with $\ddot{z}_g$, $\mu_r N$ and F_D are either not considered or negligible, the maximum horizontal acceleration responses will remain essentially constant corresponding to θ.

(2) For both isolation devices, when the roller moves within the fixed curvature range together with $\ddot{z}_g$, $\mu_r N$ and F_D are either not considered or negligible, the maximum horizontal acceleration responses are inversely proportional to R.

(3) When the roller moves apart from (or within) the fixed curvature range as well as $\mu_r N$ and F_D are not considered for simplicity, the dynamic behavior of Type A isolation device in which the roller is sandwiched between two V-shaped surfaces with a sloping angle of θ (or between two round surfaces with a curvature radius of $2R$) should be identical to that of Type B isolation device in which the roller is sandwiched between a flat surface and a V-shaped surface with a sloping angle of 2θ (or between a flat surface and a round surface with a curvature radius of R).

(4) All the equations omitting F_D can be used to represent the dynamic behavior of both isolation devices when the supplemental sliding friction is not provided.

3.2. Simplified twin-flag hysteretic model

The hysteresis behavior of the sloped multi-roller isolation devices with and without built-in sliding friction mechanisms subjected to horizontal excitations can be simulated by a simplified twin-flag hysteretic model consisting of "Multi-Linear Elastic" model and "Plastic (Wen)" model (Wen 1976) in the readily available analysis programs, as illustrated in Figure 2. When the roller moves within the fixed curvature range d, the first slopes of "multi-linear elastic" models of Type A and Type B isolation devices are determined to be $Mg/2R$ and $Mg/4R$, respectively, according to Equations (1) and (3). After the roller moves apart from the fixed curvature range, the second slopes of "multi-linear elastic" models of Type A and Type B isolation devices are perfectly plastic with constant levels of $Mg\sin 2\theta/2$ and $Mg\sin\theta/2$, respectively, according to Equations (2) and (4). No matter when the roller moves within or apart from the fixed curvature range d, the characteristic strengths of "Plastic (Wen)" models for Type A and Type B isolation devices can be simplified to be equal to $\mu_r N + F_D$ (or $\mu_r N$ if the supplemental sliding friction is not provided).

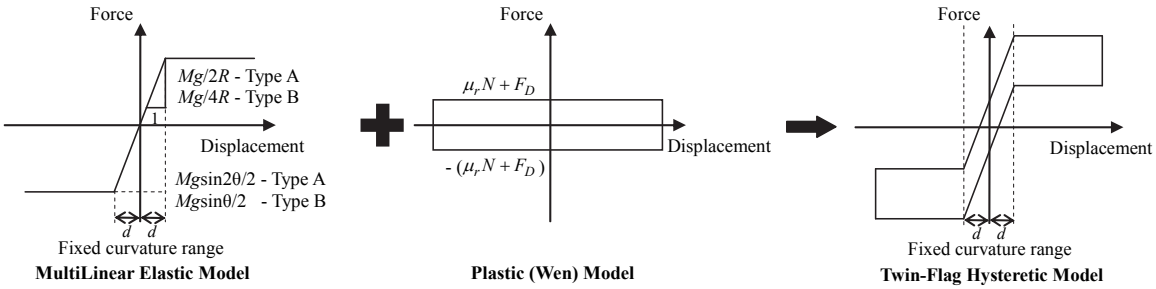

Figure 2: Simplified mathematical hysteretic models of sloped multi-roller isolation devices.

4. SEISMIC SIMULATION TEST

4.1. Test models

The maximum allowable displacement of the tested sloped multi-roller isolation devices is designed to be 250*mm*. An arc length of 19*mm* with a curvature radius (R) of 100*mm* is provided at the intersection of two inclines of the V-shaped surfaces of the bearing plates. The supplemental friction damping mechanism is composed of the rubber pad with a thickness of 2*mm* vulcanized and attached to the surfaces of the bearing plates sliding against the stainless steel surface of the side plate. In Test Scheme I, as shown in Figure 3, four sloped multi-roller isolation devices, as detailed in Table 1, are designed to investigate the effects of different design parameters on the seismic performance of the isolation devices. The to-be-protected equipment above the isolation devices is simulated by lead blocks with a total mass of 500N-sec^2/m. In Test Scheme II, as shown in Figure 4, the effectiveness of Type B isolation devices with the supplemental friction mechanism is investigated for a seismically isolated raised floor system with a plane dimension of 3m by 3m. The sloping angle (θ) is designed to be 6 degrees. A total mass of the raised floor system is about 1420N-sec^2/m. The to-be-protected equipment above the isolated raised floor system is simulated by lead blocks with a total mass of 1000N-sec^2/m.

Table 1: Design parameters of different sloped multi-roller isolation devices in Test Scheme I

Bearing No.	Bearing type	Design parameter		
		Sloping angle of V-shaped surface		Normal force for sliding friction force applied on each side plate
		Upper and lower bearing plates	Intermediate bearing plate	
A-1	A	6.25 degrees	6.25 degrees	w/o
A-2	A	6.25 degrees	6.25 degrees	332.52N
B-1	B	flat	6.25 degrees	w/o
B-2	B	flat	6.25 degrees	332.52N

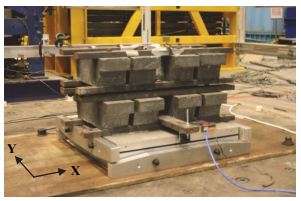

(a) Type A (A-1 and A-2)

(b) Type B (B-1 and B-2)

Figure 3: Installation of test models in Test Scheme I.

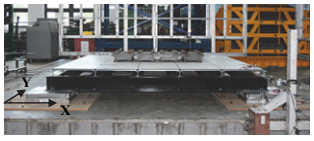

Figure 4: Installation of isolated raised floor system in Test Scheme II.

4.2. Input ground motions

As summarized in Table 2, one recorded ground motion, the 1940 El Centro earthquake denoted as I-ELC270 thereafter, is used for the seismic simulation test. In addition, two generated acceleration histories, denoted as AC156-TAP090 and AC156-TCU054 thereafter, compatible with the required response spectra (RRS) are also adopted in the test. The RRS determined are based on the Taiwan seismic design specifications and AC156 [AC156 2007].

Table 2: Acceleration excitation program

Test name		Input earthquake information or response spectrum condition	Excitation direction		Targeted input peak acceleration (g)
Recorded earthquake history	I-ELC270	El Centro, Imperial Valley, U.S. 1940/05/19	Unilateral	X	0.36
			Bilateral	X/Y	0.36/0.21
Artificial acceleration history	AC156-TAP090	Near TAP090 station, 7-story structure, 24m in height, isolated equipment is placed at 3rd floor (8.75m in elevation)	Unilateral	X	0.50
			Bilateral	X/Y	0.50/0.45
	AC156-TCU054	Near TAP054 station, 3 story structure, 12m in height), isolated equipment is placed at 3rd floor (8m in elevation)	Unilateral	X	1.00
			Bilateral	X/Y	1.00/0.96

4.3. Seismic Responses

In Test Scheme I, the comparisons of seismic responses for Bearings A-1, A-2, B1 and B2 subjected to unilateral I-ELC270 are illustrated in Figure 5. The increase of supplemental sliding friction mechanism will lead to the reduction of maximum horizontal displacement responses but will also result in the augment of maximum horizontal acceleration responses. In addition, the oscillation after input excitations will be damped out more quickly. Assuming the rolling friction contribution is very limited, the maximum horizontal acceleration response of Bearing A-1 is larger than and about twice ($\sin(2\theta)/\sin(\theta) \approx 2$ in which θ is 6.25 degrees) as that of Bearing B-1. More importantly, the test results show that the maximum horizontal displacement response of Type B isolation device is less than that of Type A isolation device, which implies that the increase in sloping angles of bearing plates (or potential energy capability) may not result in the reduction of maximum horizontal displacement responses of the isolation device. It can be clarified using the definition of equivalent damping ratios. When Type A and Type B isolation devices have the same horizontal displacement responses, the calculated equivalent damping ratio of Type B isolation device is more significant than that of Type A isolation device due to the smaller strain energy of Type B isolation device. In Test Scheme II, the X directional acceleration response histories transmitted to the isolated raised floor system and the X directional hysteresis loops of the isolated raised floor system under bilateral AC156-TCU054 are depicted in Figure 6. It can be seen that the maximum transmitted acceleration response can be drastically reduced in comparison with the input peak acceleration and can still reveal an acceptably steady level. Besides, the hysteresis loops reveal a better energy dissipation capability since the supplemental sliding friction is engaged.

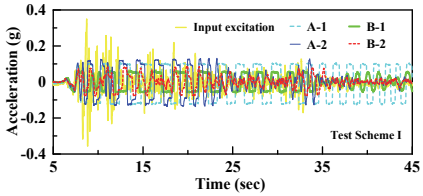

(a) acceleration response history

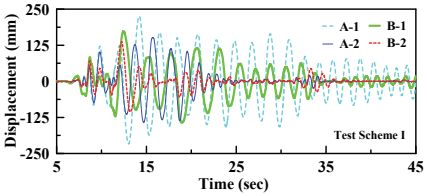

(b) displacement response history

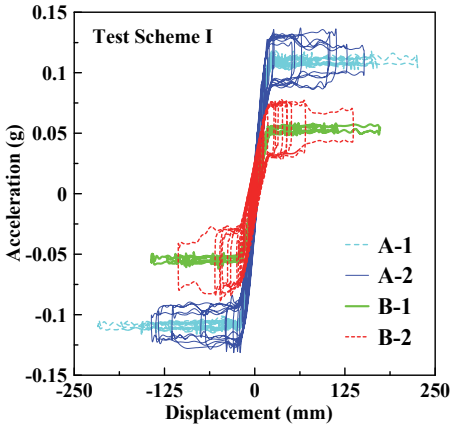

(c) hysteresis loop

Figure 5: Comparisons of seismic responses of isolation devices under unilateral I-ELC270.

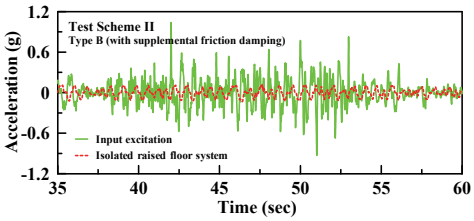

(a) X directional acceleration response history

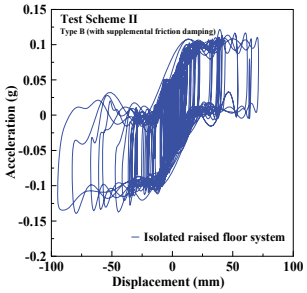

(b) X directional hysteresis loop

Figure 6: Seismic responses of isolated raised floor system under bilateral AC156-TCU054.

5. NUMERICAL VERIFICATION

Under the condition that the test models are subjected to horizontal excitations, the dynamic behavior of a single degree of freedom (SDOF) system equipped with the sloped multi-roller isolation devices can be numerically predicted using the simplified twin-flag hysteretic model, as presented in Figure 7. It is evident that the numerical predictions using the proposed simplified mathematical hysteretic models have an excellent agreement with the seismic simulation test results, including the predictions of amplitude and phase responses.

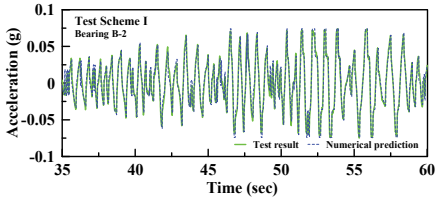

(a) acceleration response history of Bearing B-2

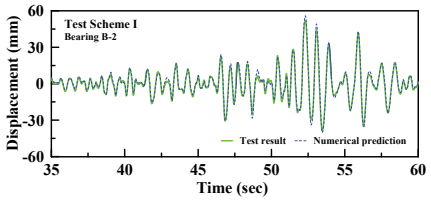

(b) displacement response history of Bearing B-2

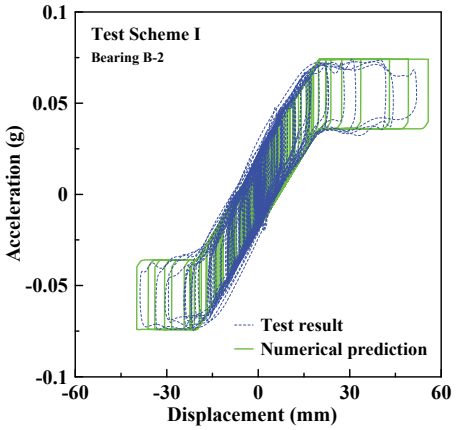

(c) hysteresis loop of Bearing B-2

Figure 7: Comparisons of experimental results and numerical predictions under unilateral AC156-TAP090.

6. CONCLUSIONS

The sloped multi-roller isolation device has numerous advantages in which the zero post-elastic stiffness performance is the most attractive feature. The dynamic behavior of the isolation device is discussed in this paper. A simplified twin-flag hysteretic model is then proposed to represent the hysteresis behavior of the isolation device. Seismic simulation tests on the isolation devices with different design parameters and an isolated raised floor system were also conducted. The high efficiency of employing the isolation devices in reducing seismic damage potential of the protected objects is experimentally verified. A satisfactory agreement between test results and numerical predictions shows the validity and practical applicability of the proposed twin-flag mathematical model in characterizing the hysteresis behavior of the isolation devices.

REFERENCES

AC156 (2007), Acceptance Criteria for Seismic Qualification by Shake-table Testing of Nonstructural Components and Systems. ICC Evaluation Service inc.

CRS, Cosine Curved Rail System. http://www.oiles.co.jp/en/menshin/building/ units/crs.html.

Hwang JS, Huang YN, Hung YH and Huang JC (2004). Applicability of seismic protective systems to structures with vibration sensitive equipment. Journal of Structural Engineering, ASCE, 130(11), pp. 1676-1684.

Ismail M, Rodellar J and Ikhouane F (2009). An innovative isolation bearing for motion-sensitive equipment. Journal of Sound and Vibration, 326, pp. 503-521.

ISO-BaseTM Seismic Isolation Platform. http://www.worksafetech.com/pages/ISO %5FBase.html.

Jangid RS and Londhe YB (1998). Effectiveness of elliptical rolling rods for base isolation. Journal of Structural Engineering, ASCE, 124, pp. 469-472.

Kasalanati A, Reinhorn AM, Constantinou MC and Sanders D (1997). Experimental study of ball-in-cone isolation system. Proceedings of the ASCE Structures Congress XV, Portland, Oregon, pp. 1191–1195.

Lambrou V and Constantinou MC (1994). Study of seismic isolation systems for computer floors. Technical Report, NCEER-94-0020.

Lee GC, Ou YC, Niu T, Song J and Liang Z (2010). Characterization of a roller seismic isolation bearing with supplemental energy dissipation for highway bridges. Journal of Structural Engineering, ASCE, 136(5), pp. 502-510.

Lin TW and Hone CC (1993). Base isolation by free rolling rods under basement. Earthquake Engineering and Structural Dynamics, 22, pp. 261-73.

Lu LY and Lin GL (2008). Predictive control of smart isolation system for precision equipment subjected to near-fault earthquakes. Engineering Structures, 30, pp. 3045-3064.

Tsai MH, Wu SY, Chang KC and Lee GC (2007). Shaking table tests of a scaled bridge model with rolling type seismic isolation bearings. Engineering Structures, 29(9), pp. 694-702.

Wang SJ, Hwang JS, Chang KC, Tsai MS, Shiau CY and Yu CH (2012). Development of sloped rolling-type isolation devices for seismic protection of important equipment and facilities. Proceedings of the 15th World Conference on Earthquake Engineering (15WCEE), Lisbon, Portugal.

Wen YK (1976). Method for random vibration of hysteretic systems. Journal of Engineering Mechanics, ASCE, 102(2), pp. 249-263.